RESEARCH PAPER

Low-level ^{40}Ca determinations using nitrous oxide with reaction cell inductively coupled plasma–tandem mass spectrometry

Shaun T. Lancaster[1] · Thomas Prohaska[1,2] · Johanna Irrgeher[1,2]

Abstract

In inductively coupled plasma mass spectrometry, the most abundant Ca isotope (^{40}Ca) suffers from isobaric interference with argon, hindering the potential for low detection limits of Ca. A powerful approach is to remove the interference by using a reaction gas in a reaction cell. Ammonia (NH_3) has proven to be an effective reaction gas by process of a charge transfer reaction. However, NH_3 is highly corrosive and toxic and cannot remove isobaric ^{40}K. Therefore, this work proposes the use of nitrous oxide (N_2O) to mass shift the target analyte ^{40}Ca to ^{40}Ca^{16}O$^+$ as a non-corrosive and non-toxic alternative. Instrument performance testing demonstrated that N_2O was capable of reaching equivalent detection limits (0.015 ng g^{-1}) and background equivalence concentrations (0.041 ng g^{-1}) to that of NH_3 and limited by the blank only. Further investigation of matrix interferences with synthetic standards highlighted that the N_2O approach supports the separation of potassium (K) and magnesium (Mg)–based interferences at tested concentrations of more than 600 times and almost 800 times higher than Ca respectively, whereas NH_3 was found to only support the removal of Mg. This work highlights a clear advantage of N_2O for low-level Ca determinations with high matrix loads, as well as compatibility with other instrumentation sensitive to corrosion that supports reaction cell technology.

Keywords Calcium · ICP-MS/MS · N_2O · Mass shift

Introduction

Inductively coupled plasma mass spectrometry (ICP-MS) is a widely used tool that boasts high sensitivity, low limit of detection (LOD), and high sample throughput. However, LODs of ICP-MS measurements can suffer due to spectral interferences from monatomic or polyatomic ions with the same mass to charge ratio (m/z). Calcium (Ca) is an example of an element that suffers from such interferences. In this case, the major isotope, ^{40}Ca, which has a natural abundance of 96.941% [1], shares an isobaric interference with argon

✉ Johanna Irrgeher
  johanna.irrgeher@unileoben.ac.at

1 Department of General, Analytical and Physical Chemistry, Chair of General and Analytical Chemistry, Montanuniversität Leoben, 8700 Leoben, Austria

2 Department of Physics and Astronomy, University of Calgary, Calgary, Canada

(Ar), which is used as both a carrier gas and for the generation of the plasma. To separate these, the required mass resolution would be > 190,000 (Table 1). As such, sensitivity and detection limits are greatly hampered by resorting to using less abundant Ca isotopes, such as ^{42}Ca (0.647% abundance), ^{43}Ca (0.135% abundance), and ^{44}Ca (2.086% abundance) [1].

One method commonly employed to overcome spectral interferences is the introduction of a reaction gas via a reaction cell. Recently developed instruments utilize an additional quadrupole as a mass filter in front of the reaction cell to avoid the formation of new interferences in the cell (ICP–tandem mass spectrometry (MS/MS)) [2, 3]. Ammonia (NH_3) has been typically used as a reaction gas to remove interference of ^{40}Ar$^+$ for on-mass determination of ^{40}Ca$^+$ [4], as the charge transfer reaction ($M^+ + NH_3 \rightarrow NH_3^+ + M$) occurs at a much higher rate for Ar$^+$ than for Ca$^+$ [2, 5, 6]. However, NH_3 is a corrosive and toxic gas [7]. Therefore, it cannot be used in every instrument and its usage is sometimes limited in some laboratories. It is therefore of interest to assess suitable alternatives for greater sustainability regarding primarily the protection of the instrumentation.

Other reaction gases have also been used for on-mass determinations of ^{40}Ca, such as methane [8, 9] and hydrogen [10]. However, mass-shift reactions of ^{40}Ca using a reaction gas (e.g. $^{40}Ca \rightarrow ^{40}Ca^{16}O^+$) are less widely reported. Oxygen is the traditional reaction gas for analyte mass-shift determinations [2]. However, low formation of the CaO^+ product ion renders this approach unfavourable [11]. Nitrous oxide (N_2O), on the other hand, is a more reactive alternative to oxygen [12, 13] and has been explored recently for a number of elements using ICP-MS/MS systems [14–16], highlighting a broad scope for use in routine multi-element analysis. While N_2O shows high reactivity, it is notably much less corrosive than NH_3 and may serve as a suitable alternative. Apart from ^{40}Ar, other interferences have to be considered if Ca is determined at low levels in a complex matrix (see Table 1).

While sensitivity can be enhanced and the LOD can be decreased by using cell methodology, it is important to note that current LODs are limited by background levels of Ca. Therefore, it is important to be highly considerate of sources of contamination. Wu et al. suggested the use of a clean laboratory environment can allow for lower detection limits [9]. Retzmann et al. described in detail how to minimize the Ca background and reported that, e.g., the use of nitrile gloves and clean-room wipes were major sources of Ca contamination and should be avoided [17].

This work aims to evaluate the novel usage of N_2O for quantification of Ca at low levels in complex matrices by ICP-MS/MS using ^{40}Ca. Optimization of both the cell gas flow rates and possible internal standards was carried out. Instrument performance parameters for both reaction gases (NH_3 and N_2O) were compared with each other, as well as with the determination of ^{40}Ca under standard conditions (no cell gas). Additionally, the effectiveness of the removal of sample matrix interferences caused mainly by

Table 1 List of interferences for Ca on *m/z* 40. Mass resolution was calculated from IUPAC Periodic Table of the Elements and Isotopes [1]. Negative resolutions indicate that the atomic mass of the interfering species is greater than that of.^{40}Ca

Interference on $^{40}Ca^+$	Abundance (%)	Atomic mass (u)	Required mass resolution
$^{40}Ca^+$	96.9	39.943	–
$^{40}Ar^+$	99.6	39.962	192,058
$^{40}K^+$	0.0117	39.964	− 28,394
$^{24}Mg^{16}O^+$	78.8	39.980	− 2302
$^{80}Se^{++}$	49.6	39.958	9229
$^{80}Kr^{++}$	2.29	39.958	9079
$^{39}K^1H^+$	93.2	39.972	− 4471
$^{23}Na^{17}O^+$	0.038	39.989	− 1520

magnesium (Mg) and potassium (K) was also investigated for each cell gas.

Materials and methods

All preparations and measurements were made in a clean room (ISO class 8) to minimize the risks of contamination. Polyethylene gloves (Carl Roth GmbH, Karlsruhe, Germany) were used on top of nitrile gloves to avoid Ca contamination. The use of clean-room wipes and paper towels were avoided throughout.

Chemicals and standards

Nitric acid ($w = 65\%$, p.a. grade; Carl Roth GmbH) was first purified by sub-boiling using a sub-boiling distillation system (Savillex DST-4000, AHF Analysentechnik, Tübingen, Germany). Reagent grade I water (18.2 MΩ cm; MilliQ IQ 7000, Merck-Millipore, Darmstadt, Germany) was used for all acid dilutions. Sample vials and pipette tips were pre-cleaned by soaking overnight in diluted sub-boiled nitric acid ($w = 10\%$ and subsequently $w = 3\%$ respectively) before use.

All standards were prepared in dilute sub-boiled acid ($w = 2\%$). A Ca single element ICP-MS standard ($\beta = 1000$ µg mL^{-1}; CertiPur, Merck, Darmstadt, Germany) was used as stock for calibration preparations. Single element standards of scandium (Sc, $\beta = 1000$ µg mL^{-1}; Inorganic Ventures, Christiansburg, VA, USA), yttrium (Y, $\beta = 10$ µg mL^{-1}; Elemental Scientific, Omaha, NE, USA), and indium (In, $\beta = 1000$ µg mL^{-1}; CertiPur, Merck) were used to produce a mixed internal standard. Additional 1000 µg mL^{-1} single element ICP-MS standards of magnesium ($\beta = 1000$ µg mL^{-1}; CertiPur, Merck) and potassium ($\beta = 1000$ µg mL^{-1}; CertiPur, Merck) were used for interference testing.

ICP-MS/MS measurements

All ICP-MS/MS measurements were carried out using a NexION 5000 (Perkin Elmer, Waltham, MA, USA), which is equipped with a dynamic reaction cell (DRC). Instrumental parameters are listed in Table 2. The sample was introduced to the ICP via a peristaltic pump. A mixed internal standard containing Sc ($w = 4.7$ ng g^{-1}), Y ($w = 2.2$ ng g^{-1}), and In ($w = 2.2$ ng g^{-1}) was added online. Measurement parameters for the internal standards are displayed in Table 3. Calibrations in standard mode (both using single-quadrupole mode (Q3) and MS/MS mode) were carried out in the range of 5–1000 ng g^{-1} Ca and measured using the ^{44}Ca isotope. DRC calibrations were

Table 2 Instrument and plasma conditions for measurements made using ICP-MS/MS

Parameter	Q3	MS/MS	NH₃ DRC MS/MS	N₂O DRC MS/MS
Measurement mode	Standard	Standard	DRC on mass	DRC mass shift
Cell gas	None	None	NH_3	N_2O
Cell gas flow rate	None	None	0.7 mL min⁻¹	0.4 mL min⁻¹
RPa	0	0	0	0
RPq	0.25	0.25	0.45	0.45
Sample introduction	Peristaltic pump	Peristaltic pump	Peristaltic pump	Peristaltic pump
Nebulizer	PFA MicroFlow	PFA MicroFlow	PFA MicroFlow	PFA MicroFlow
Spray chamber	Peltier cooled SilQ cyclonic spray chamber	Peltier cooled SilQ cyclonic spray chamber	Peltier cooled SilQ cyclonic spray chamber	Peltier cooled SilQ cyclonic spray chamber
Spray chamber temperature	5 °C	5 °C	5 °C	5 °C
Interface cones	Nickel	Nickel	Nickel	Nickel
RF power	1600 W	1600 W	1600 W	1600 W
Ar nebulizer gas flow	0.98 L min⁻¹	0.98 L min⁻¹	0.98 L min⁻¹	0.98 L min⁻¹
Ar auxiliary gas flow	1.2 L min⁻¹	1.2 L min⁻¹	1.2 L min⁻¹	1.2 L min⁻¹
Ar plasma gas flow	16 L min⁻¹	16 L min⁻¹	16 L min⁻¹	16 L min⁻¹
QID fixed voltage	− 12 V	− 12 V	− 12 V	− 12 V
Hyperskimmer park voltage	5 V	5 V	5 V	5 V
OmniRing park voltage	− 185 V	− 185 V	− 185 V	− 185 V
Inner target lens voltage	2 V	2 V	2 V	2 V
Outer target lens voltage	− 7 V	− 7 V	− 7 V	− 7 V
Deflector exit voltage	− 8 V	− 8 V	− 8 V	− 8 V
Differential aperture voltage	− 3.5 V	− 3.5 V	− 3.5 V	− 3.5 V
Q1 AC rod offset	− 7 V	− 6 V	− 5 V	− 7.5 V
Q1 rod offset	− 11 V	− 2 V	− 0 V	0 V
Cell rod offset	− 33 V	− 33 V	− 5 V	− 2 V
Axial field voltage	0 V	0 V	150 V	250 V
Cell entrance voltage	− 10 V	− 5 V	− 6.5 V	− 7.5 V
Cell exit voltage	− 2 V	− 2 V	− 7 V	− 5 V
Q3 AC rod offset	− 2.5 V	− 2.5 V	− 8.5 V	− 8 V
Q3 rod offset	− 2 V	− 2 V	− 13 V	− 10 V
Dwell time	50 ms	50 ms	50 ms	50 ms
Scans	6	6	6	6
Replicates	6	6	6	6

Table 3 ICP-MS/MS measurement conditions for the tested internal standards using N₂O and NH₃ DRC

Internal standard	Reaction gas	Q1 m/z	Q3 m/z
Sc	N_2O	45	61
Y	N_2O	89	105
In	N_2O	115	115
Sc	NH_3	45	45
Y	NH_3	89	89
In	NH_3	115	115

carried out in the range of 0.2–100 ng g⁻¹ Ca and measured using both the ⁴⁰Ca and ⁴⁴Ca isotopes. Using N_2O, Ca was detected as the $^{40}Ca^{16}O^+$ and $^{44}Ca^{16}O^+$ product ions (mass shift of +16 amu).

Cell gas flow rate optimization

Optimization of the reaction gas flow rates for NH_3 and N_2O was carried out on m/z 40 using a 10-ng g⁻¹ single element Ca standard and a blank solution ($w = 2\%$ HNO₃). Tested flow rates ranged from 0.1 to 1.0 mL min⁻¹ using N_2O and from 0.4 to 1.5 mL min⁻¹ using NH_3.

Evaluation of matrix interferences

Evaluation of potential interference caused by Mg and K using N_2O and NH_3 DRC was carried out by measurement of the Ca background equivalence concentration in each respective single element standard at dilutions between 0.5 and 5.0 µg g^{-1}. Determined Ca concentrations, made by means of external calibration, were used to evaluate the significance of each interference by comparing the mass fraction of Ca obtained using the non-interfered (by isobaric interference) isotope on m/z 44 ($w(Ca)_{m/z\ 44}$) to that of the interfered isotope on m/z 40 ($w(Ca)_{m/z\ 40}$). Where the difference was found to be significant, the magnitude of interference was calculated by subtraction of $w(Ca)_{m/z\ 44}$ from $w(Ca)_{m/z\ 40}$.

Certified reference materials

River water certified reference materials (CRMs), SLRS-3 and SLRS-5 (both National Research Council Canada, Ontario, Canada), were used for validation. The materials were diluted to approximately 1 ng mL^{-1} Ca using dilute sub-boiled acid ($w = 2\%$ HNO_3). Analysis was carried out using N_2O and NH_3 as reaction gases.

Statistics

Statistical testing and the generation of figures were carried out using RStudio (version 2021.9.2.382). LOD and LOQ were calculated respectively from 3 and 10 times the standard deviation of 5 repeated measurements of a blank solution ($w = 2\%$ HNO_3). Background equivalence concentration (BEC) was calculated from the calibration by division of the background (y-intercept) with the calibration slope. Equidistant standard concentrations of Ca between 0.2 and 1.0 ng g^{-1} were used when determining the LOD, LOQ, and BEC of the DRC methods.

Evaluation of the effect of interferences was carried out using total least squares (Deming) regression on the concentrations obtained using the ^{40}Ca and ^{44}Ca isotopes, where standard errors were calculated using the jackknife method. The observed $w(Ca)_{m/z\ 40}/w(Ca)_{m/z\ 44}$ ratio was statistically compared to the expected ratio of 1 using a Z test.

Results and discussion

Cell gas flow rate optimization

The profile observed for mass shift using N_2O (Fig. 1A) displayed optimum sensitivity for the formation of the $^{40}Ca^{16}O^+$ product ion at 0.4 mL min^{-1}. The background signal of $^{40}Ar^+$ was found to decrease as the N_2O flow rate increased.

Further observations of the blank signal conducted using the ^{44}Ca isotope at optimum N_2O conditions found a similar signal ratio of $^{40}Ca/^{44}Ca$ to that of the natural abundance. This suggests that, while a small degree of $^{40}Ar^{16}O^+$ forms at lower N_2O flow rates, Ar was successfully removed by N_2O at optimum conditions and the observed blank signal is primarily due to the presence of background Ca.

On-mass determination of Ca was carried out using NH_3 flow rates between 0.4 and 1.5 mL min^{-1}, as preliminary tests (carried out using ^{38}Ar) suggested that lower flow rates would not remove enough Ar to prevent detector saturation on m/z 40. Within this range, the signal for Ca was observed to decrease with increasing NH_3 flow (Fig. 1B).
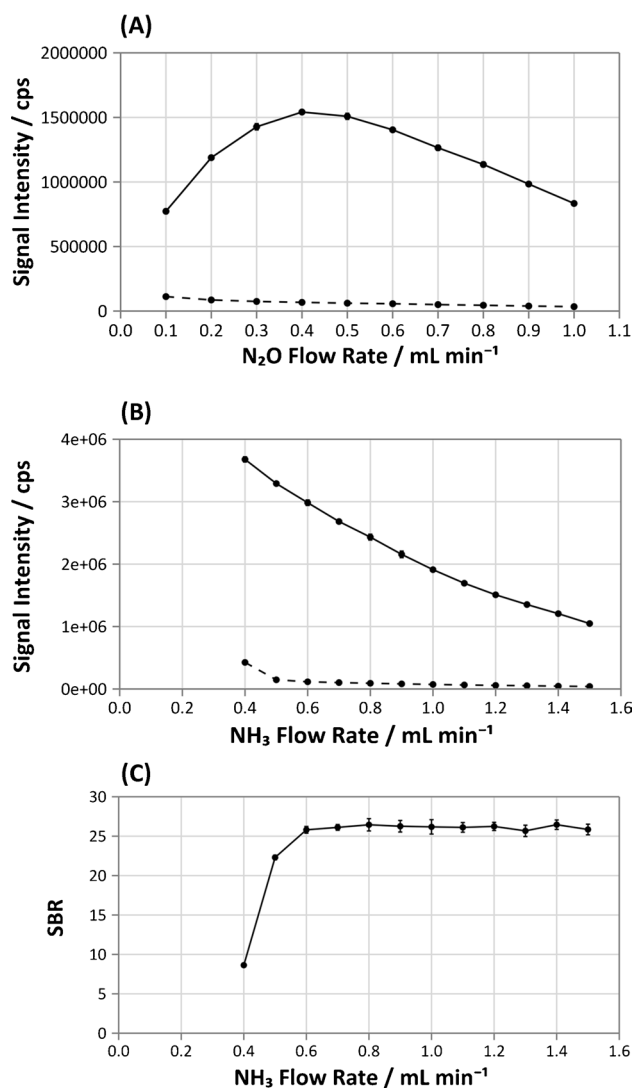

Fig. 1 Optimization of sensitivity for 10 ng g^{-1} Ca (solid line) using **A** N_2O and **B** NH_3 cell gas flow rate for the removal of ^{40}Ar interference on.^{40}Ca. The background signal, measured using a blank solution, is also indicated (dotted line). Variation in the signal to background ratio (SBR) for NH_3 DRC is shown in **C**. Error bars present represent one standard deviation of six replicates

Consideration of the signal to background ratio demonstrated a plateau at NH$_3$ flow rates greater than 0.7 mL min^{-1} (Fig. 1C); hence, this was determined to be the optimum condition. Similar to the use of N$_2$O DRC, additional monitoring of the blank using ^{44}Ca highlighted that the blank signal obtained on m/z 40 at the optimum NH$_3$ flow rate was due to the presence of background Ca.

Internal standards

Sc, Y, and In were tested as possible internal standards, as they have a narrow range of ionization energies (5.78–6.56 eV) close to that of Ca (6.11 eV) [18]. Variation of the internal standard response to the DRC gas flow rate is shown in Fig. 2. Initial tests using N$_2$O DRC highlighted that In could not be measured in mass-shift mode, as no formation of the InO$^+$ product ion was observed. However, detection of In$^+$ on mass with N$_2$O was found to be feasible, as an adequate and stable signal was obtained. Given that the sensitivity of the In signal increased with N$_2$O flow rates up to 0.7 mL min^{-1}, it could be interpreted that the signal observed may be enhanced by collisional focussing. Sc and Y, on the other hand, were observed to form the oxide product ion. Additionally, the sensitivity profiles closely matched that of Ca, with both internal standards displaying

Fig. 2 Variation of ^{45}Sc (solid line), ^{89}Y (dashed line), and.^{115}In (dotted line) internal standard signal with **A** N$_2$O and **B** NH$_3$ cell gas flow rate. Error bars present represent one standard deviation of six replicates

an optimum N$_2$O flow rate of 0.4 mL min^{-1}. The use of Sc and Y may then prove more advantageous in comparison to In, as they display similar cell reaction characteristics to that of the analyte.

In contrast, Sc and Y were observed to be unfit for use as internal standards when using NH$_3$ as a reaction gas (Fig. 2B), as both elements were effectively removed when measuring on mass. The profile of In showed a collisional focussing effect, where a sufficient and stable signal was obtained for use as an internal standard at the previously determined optimum NH$_3$ flow rate of 0.7 mL min^{-1}. Given that, of the three internal standards considered, In was the only one found to be suitable for measurements, all subsequent data reported for NH$_3$ DRC only includes internal normalization to In.

Performance data

The instrument performance for the two DRC methods, as well as standard mode, was assessed and is presented in Table 4. Between the three internal standards used for N$_2$O DRC, minimal differences in sensitivity (slope = 128,000–129,000 cps/ng g^{-1}) and BEC (0.41–0.42 ng g^{-1}) were observed. However, stability data indicated a lower RSD when using Sc (1.6%) as an internal standard compared to Y (2.2%) and In (2.9%). This was also reflected in the slightly lower LOD (of 0.015 ng g^{-1}) and LOQ (of 0.049 ng g^{-1}) values obtained using Sc. Therefore, while all three internal standards can be used for determination of Ca, Sc has been shown here to be the optimal in this case.

While the calibration slope observed for ^{40}Ca using NH$_3$ was 1.75 times greater than that of the N$_2$O, the LOD (of 0.015 ng g^{-1}) and LOQ (of 0.049 ng g^{-1}) remained consistent. Additionally, determined BEC values (of 0.37 ng g^{-1} and 0.41 ng g^{-1} for NH$_3$ and N$_2$O DRC respectively) were similar between the two methods. This further indicates that the background signal for both DRC methods is likely due to background Ca levels. In comparison to the measurement of ^{44}Ca using the Q3 mode with no cell gas (which is more sensitive than the MS/MS mode with no cell gas), the application of both NH$_3$ and N$_2$O DRC methods showed marked improvement, with approximately 10 times lower LOD (of 0.015 ng g^{-1}) and LOQ (of 0.049 ng g^{-1}), and approximately 45 times lower BEC (of 0.42 ng g^{-1}).

Removal of interferences

Mg and K were identified as the primary interferences of concern for measurements using the ^{40}Ca isotope, as the polyatomic ^{24}Mg^{16}O$^+$ interference formed in the plasma and isobaric interference from ^{40}K$^+$ cannot be removed by the Q1 mass filter. Selenium, as ^{80}Se^{++}, was not considered to

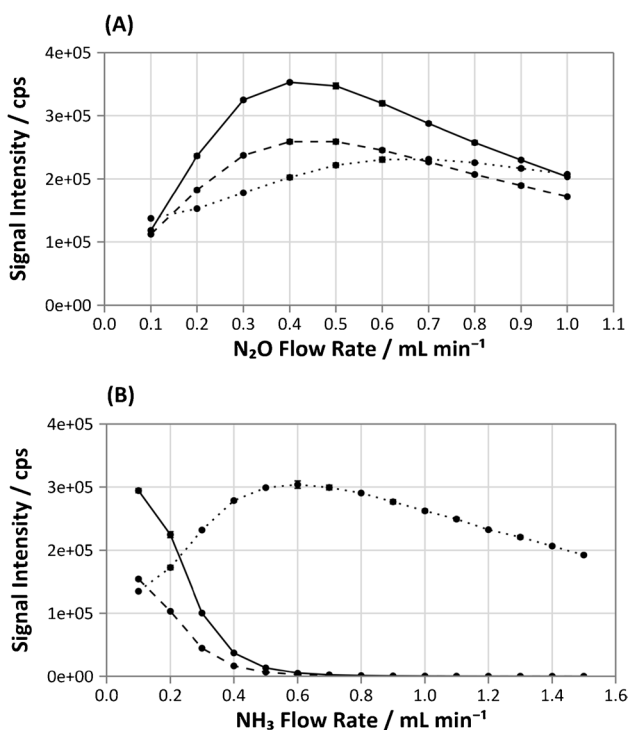**Table 4** Comparison of calibration parameters for the measurement of ^{44}Ca with no reaction gas in Q3 and MS/MS mode, and ^{40}Ca in MS/MS mode with N_2O and NH_3 reaction gas

Parameter	^{44}Ca Q3 mode (no cell gas)	^{44}Ca MS/MS mode (no cell gas)	^{40}Ca on mass NH_3 DRC	^{40}Ca mass shift N_2O DRC	^{40}Ca mass shift N_2O DRC	^{40}Ca mass shift N_2O DRC
Internal standard	Indium	Indium	Indium	Scandium	Yttrium	Indium
Slope (cps/ng g^{-1})	8260	3650	226,000	129,000	129,000	128,000
Intercept (cps)	150,000	56,500	82,500	52,600	52,700	53,300
Correlation, R	0.99983	0.99968	0.99832	0.99941	0.99924	0.99930
LOD (ng g^{-1})	0.14	0.27	0.015	0.015	0.017	0.017
LOQ (ng g^{-1})	0.43	0.81	0.049	0.049	0.057	0.056
BEC (ng g^{-1})	18	15	0.37	0.41	0.41	0.42
Stability test accuracy (%)*	–	–	101	101	99.3	97.0
Stability test RSD (%)*	–	–	2.39	1.57	2.20	2.92

*Based on 20 replicate measurements of a 0.5-ng g.$^{-1}$ Ca standard

be of concern due to the high ionization energy required to form such interfering species [18] (Table 5).

Native Ca concentrations in the measured single element standards of both Mg and K ranged between 1 and 10 ng g^{-1}. For measurements of Ca with high Mg load, the $w(Ca)_{m/z\ 40}/w(Ca)_{m/z\ 44}$ ratio did not significantly differ from 1 for both N_2O and NH_3, which indicates that both gases can achieve successful removal of $^{24}Mg^{16}O^+$ interference on m/z 40. However, measurements of native Ca in high-level K standards using NH_3 DRC showed a significantly greater $w(Ca)_{m/z\ 40}/w(Ca)_{m/z\ 44}$ ratio than expected, indicating significant bias introduced due to the presence of interfering ^{40}K that was not removed. Conversely, no such significant bias was observed for measurements of K single element

standards using N_2O DRC, suggesting that N_2O can be used to successfully overcome the interference of K.

The level of interference from ^{40}K using NH_3 DRC was determined by the difference of the observed $w(Ca)_{m/z\ 40}$ and $w(Ca)_{m/z\ 44}$ and plotted against the prepared K concentration (Fig. 3). The slope of the plot indicated that the level of interference on ^{40}Ca appears as 0.0128% of the matrix K concentration. To obtain < 1% interference on ^{40}Ca, matrix K concentrations cannot exceed about 80 times that of the analyte Ca concentrations. Further variation of the NH_3 flow rate was not able to overcome the isobaric interference from K, as the Ca/K signal ratio only decreased with increasing flow rate (Fig. 4).

Table 5 Total least squares regression results for the comparison of determined background Ca concentrations ($w = 0$–7.5 ng g^{-1}) using isotopes ^{44}Ca and ^{40}Ca in high-concentration Mg ($w = 0$–4.0 μg g^{-1}) and K ($w = 0$–4.4 μg g.$^{-1}$) single element standards

DRC mode	Slope $w(Ca)_{m/z\ 40}$ vs. $w(Ca)_{m/z\ 44}$	Standard error of the slope	Z test p value	Significant?	Lower confidence interval	Upper confidence interval
Potassium interference						
N_2O at 0.4 mL min^{-1} (Sc Int. Std.)	0.9917	0.0062	> 0.150	No	0.96518	1.01825
N_2O at 0.4 mL min^{-1} (Y Int. Std.)	0.9916	0.0061	> 0.150	No	0.96532	1.01797
N_2O at 0.4 mL min^{-1} (In Int. Std.)	0.9915	0.0061	> 0.150	No	0.96526	1.01777
NH_3 at 0.7 mL min^{-1} (In Int. Std.)	1.1335	0.0022	< 0.001	Yes	1.12386	1.14314
Magnesium interference						
N_2O at 0.4 mL min^{-1} (Sc Int. Std.)	0.9982	0.0107	> 0.150	No	0.95212	1.04429
N_2O at 0.4 mL min^{-1} (Y Int. Std.)	0.9986	0.0111	> 0.150	No	0.95084	1.04626
N_2O at 0.4 mL min^{-1} (In Int. Std.)	0.9987	0.0104	> 0.150	No	0.95399	1.04336
NH_3 at 0.7 mL min^{-1} (In Int. Std.)	1.0062	0.0128	> 0.150	No	0.95135	1.06103
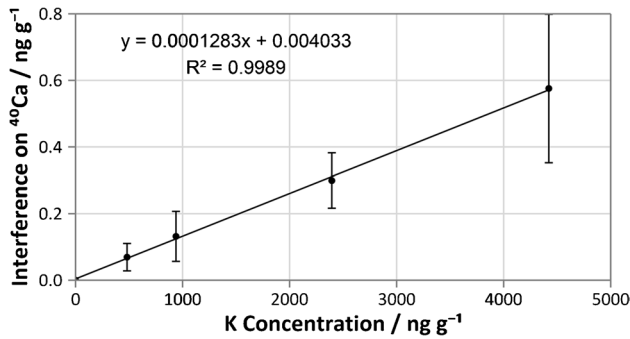
Fig. 3 Contribution of ^{40}K interference on ^{40}Ca measurements of single element K standards ($w=0$–4.4 µg g.$^{-1}$) using NH$_3$ DRC. Error bars present represent the combined standard deviation of the difference between the observed $w(Ca)_{m/z\ 40}$ and $w(Ca)_{m/z\ 44}$ (calculated by the law of propagation of uncertainties)

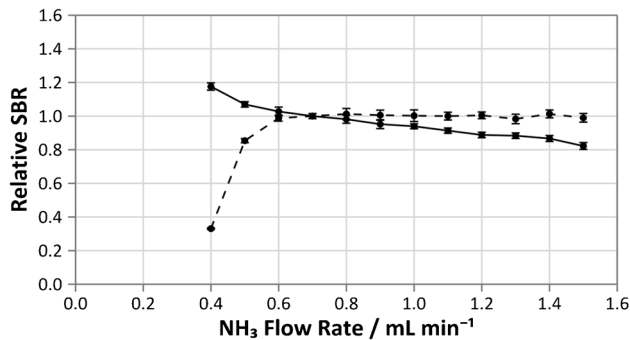**Fig. 4** Variation of the relative signal to background ratio (SBR) with NH$_3$ flow rate (normalized to the SBR observed at 0.7 mL min^{-1} NH$_3$) for 10 ng g^{-1} ^{40}Ca signal with a 25 ng g^{-1}.^{39} K background (solid line) and blank background on m/z 40 (dotted line). Error bars represent one combined standard deviation of six replicates (calculated by the law of propagation of uncertainties)

Method validation

Validation of the total determination of Ca using N$_2$O DRC was carried out using two river water CRMs that were certified for Ca. Results are shown in Table 6. Excellent recoveries between 99.2 and 103% were obtained for the two CRMs using Sc and Y as internal standards. Slightly lower recoveries of 95.4–96.9% were obtained using In as an internal standard, though these still fall within the stated uncertainty of the CRM. Recoveries of 97.9–98.5% were obtained using NH$_3$ DRC, indicating that the N$_2$O DRC method for determination of total Ca performs as well as existing methodology for real sample matrices.

Conclusions

The data presented within this study suggests that N$_2$O is not only a suitable replacement for NH$_3$ for total Ca determinations, but can also ensure matrix-free determinations of ^{40}Ca, especially in K-rich matrices with low Ca content. Despite apparent lower sensitivity of the N$_2$O approach (by a factor of 1.75), detection limits and BEC were found to be similar between the two cell gases. We therefore propose that N$_2$O should be used in place of NH$_3$ for routine measurements of Ca, as well as incorporating this approach into wider multi-element analysis.

Table 6 Measured mass fractions and recoveries of river water CRMs (diluted to 1 ng mL.$^{-1}$) using N$_2$O and NH$_3$ DRC

CRM	Certified mass fraction (µg g^{-1})	N$_2$O DRC (Sc internal standard)		N$_2$O DRC (Y internal standard)		N$_2$O DRC (In internal standard)		NH$_3$ DRC (In internal standard)	
		Measured (µg g^{-1})	Recovery (%)	Measured (µg g^{-1})	Recovery (%)	Measured (µg g^{-1})	Recovery (%)	Measured (µg g^{-1})	Recovery (%)
SLRS-3	6.0±0.4	6.09±0.09	101	5.95±0.10	99.2	5.72±0.09	95.4	5.87±0.09	97.9
SLRS-5	10.5±0.4	10.8±0.1	103	10.8±0.1	103	10.2±0.1	96.9	10.3±0.1	98.5

Declarations

Conflict of interest The authors declare no competing interests.

References

1. Holden NE, Coplen TB, Böhlke JK, et al. IUPAC Periodic Table of the Elements and Isotopes (IPTEI) for the education community (IUPAC Technical Report). Pure Appl Chem. 2018;90:1833–2092.

2. Balcaen L, Bolea-Fernandez E, Resano M, Vanhaecke F. Inductively coupled plasma - tandem mass spectrometry (ICP-MS/MS): a powerful and universal tool for the interference-free determination of (ultra)trace elements - a tutorial review. Anal Chim Acta. 2015;894:7–19.

3. Bolea-Fernandez E, Balcaen L, Resano M, Vanhaecke F. Overcoming spectral overlap via inductively coupled plasma-tandem mass spectrometry (ICP-MS/MS). A tutorial review. J Anal At Spectrom. 2017;32:1660–79.

4. Boulyga SF, Klötzli U, Stingeder G, Prohaska T. Optimization and application of ICPMS with dynamic reaction cell for precise determination of 44Ca/40Ca isotope ratios. Anal Chem. 2007;79:7753–60.

5. Tanner SD, Baranov VI. Theory, design, and operation of a dynamic reaction cell for ICP-MS. At Spectrosc. 1999;20:45–52.

6. De Muynck D, Vanhaecke F. Development of a method based on inductively coupled plasma-dynamic reaction cell-mass spectrometry for the simultaneous determination of phosphorus, calcium and strontium in bone and dental tissue. Spectrochim Acta - Part B At Spectrosc. 2009;64:408–15.

7. (2020) Ammonia, anhydrous; SDS No. 000010021772 [Online], Linde, Munich, Germany. https://produkte.linde-gas.at/sdb_konform/NH3_10021772EN.pdf. Accessed 22 March 2022

8. Chen KL, Jiang SJ. Determination of calcium, iron and zinc in milk powder by reaction cell inductively coupled plasma mass spectrometry. Anal Chim Acta. 2002;470:223–8.

9. Wu MC, Jiang SJ, Hsi TS. Determination of the ratio of calcium to phosphorus in foodstuffs by dynamic reaction cell inductively coupled plasma mass spectrometry. Anal Bioanal Chem. 2003;377:154–8.

10. Poirier L, Nelson J, Leong D, Berhane L, Hajdu P, Lopez-Linares F. Application of ICP-MS and ICP-OES on the determination of nickel, vanadium, iron, and calcium in petroleum crude oils via direct dilution. Energy Fuels. 2016;30:3783–90.

11. Zhu Y, Ariga T, Nakano K, Shikamori Y. Trends and advances in inductively coupled plasma tandem quadruple mass spectrometry (ICP-QMS/QMS) with reaction cell. At Spectrosc. 2021;42:299–309.

12. Lavrov VV, Blagojevic V, Koyanagi GK, Orlova G, Bohme DK. Gas-phase oxidation and nitration of first-, second-, and third-row atomic cations in reactions with nitrous oxide: periodicities in reactivity. J Phys Chem A. 2004;108:5610–24.

13. Koyanagi GK, Bohme DK. Oxidation reactions of lanthanide cations with N2O and O2: periodicities in reactivity. J Phys Chem A. 2001;105:8964–8.

14. Klein O, Zimmermann T, Pröfrock D. Improved determination of technologically critical elements in sediment digests by ICP-MS/MS using N2O as a reaction gas. J Anal At Spectrom. 2021;36:1524–32.

15. Harouaka K, Allen C, Bylaska E, Cox RM, Eiden GC, di Vacri ML, Hoppe EW, Arnquist IJ. Gas-phase ion-molecule interactions in a collision reaction cell with triple quadrupole-inductively coupled plasma mass spectrometry: investigations with N2O as the reaction gas. Spectrochim Acta - Part B At Spectrosc. 2021;186:106309.

16. Fu L, Huang G, Hu Y, Pan F. N2O as a universal reaction gas to overcome spectral interference in determining metal impurities in Mg(TFSI)2 electrolytes for rechargeable magnesium batteries by inductively coupled plasma tandem mass spectrometry. Anal Chem. 2022;94:3035–40.

17. Retzmann A, Walls D, Miller KA, Irrgeher J, Prohaska T, Wieser ME. A double-spike MC TIMS measurement procedure for low-amount Ca isotopic analysis of limited biological tissue samples. Anal Bioanal Chem. 2022;414:675–89.

18. Lide DR (ed) (2000) Section 10: Atomic, molecular, and optical physics. In: CRC Handbook of Chemistry and Physics, 80th Edit. CRC Press, Boca Raton, FL, pp 10–175 to 10–177

Publisher's note Springer Nature remains neutral with regard to jurisdictional claims in published maps and institutional affiliations.